Selected ion flow tube cation–molecule reaction studies and threshold photoelectron photoion coincidence spectroscopy of cyclic-C5F8

Parkes, Michael A.; Ali, Sahangir; Tuckett, Richard P.; Mikhailov, Victor A.; Mayhew, Christopher

DOI:
10.1039/b704862a

Threshold photoelectron photoion coincidence spectroscopy and selected ion flow tube reactions of *cyclic*-C_5F_8

M.A. Parkes,* S. Ali, R.P. Tuckett,* V.A. Mikhailov and C.A. Mayhew

Phys. Chem. Chem. Phys., (2007) **9**, 5222-5231

DOI: 10.1039/b704862a

Published title:
Selected ion flow tube cation–molecule reaction studies and threshold photoelectron photoion coincidence spectroscopy of cyclic-C5F8

Professor Richard Tuckett (University of Birmingham) / July 2011

(Revised version after referee comments and ***final*** corrections by authors, 10.7.07 ;
corrections since version submitted and accepted by the PCCP office on 29.6.07 are shown in RED)

Selected ion flow tube cation-molecule reaction studies and threshold photoelectron photoion coincidence spectroscopy of *cyclic*-C_5F_8 [$]

Michael A. Parkes,* Sahangir Ali, and Richard P. Tuckett
School of Chemistry, University of Birmingham, Edgbaston, Birmingham, B15 2TT, U.K.

and

Victor A. Mikhailov and Chris A. Mayhew
School of Physics and Astronomy, University of Birmingham, Edgbaston, Birmingham, B15 2TT, U.K.

Number of pages : 14 Number of tables : 2 Number of figures : 4

* Author for correspondence (Fax 0121 414 4403) email map842@bham.ac.uk

[$] The HTML version of this article has been enhanced with additional colour images

---

Abstract : The product ion branching ratios and rate coefficients have been measured using a selected ion flow tube (SIFT) at 298 K for the bimolecular reactions of *cyclic*-C_5F_8 with several atomic and molecular cations. The majority of reactions occur at the collisional rate calculated by the modified average dipole orientation theory, with the exception of H_2O^+ for which the reaction efficiency is only 55 %. Apart from H_2O^+ and N^+, the similarity of the product ion branching ratios determined from threshold photoelectron photoion coincidence (TPEPICO) and ion-molecule data suggests that long-range electron transfer is the dominant mechanism for reactions involving ions with recombination energies between 12 and 17 eV. For N^+, the product ion branching ratios are very different to those produced by photoionisation; this result may be explained if some of the N-atom products are formed electronically excited. The onset of an ionisation signal of *c*-C_5F_8 measured by TPEPICO spectroscopy occurs at 12.25 ± 0.05 eV. This is much higher than the value of the first adiabatic ionisation energy determined from electron ionisation (11.24 ± 0.10 eV), He (I) photoionisation (11.30 ± 0.05 eV), and an independent high resolution threshold photoelectron spectrum (11.237 ± 0.002 eV). The ground electronic state of *c*-$C_5F_8^+$ has very weak intensity under threshold electron conditions. The TPEPICO spectrum of *c*-C_5F_8 recorded from 12–23 eV shows detection of the parent ion and the daughter ions $C_4F_6^+$ and $C_5F_7^+$, with their appearance energies increasing in this order. Ion yield curves and branching ratios have been determined. Using Gaussian 03, the enthalpy of formation of *c*-C_5F_8 at 298 K has been determined to be −1495 kJ mol^{-1}.

1. Introduction

Recently, our group completed two studies on the ion chemistry of the important industrial gas *cyclic*-C_4F_8.[1,2] One examined the positive ion chemistry using threshold photoelectron photoion coincidence (TPEPICO) spectroscopy and a selected ion flow tube (SIFT).[1] The other investigated negative ion formation *via* electron attachment.[2] *c*-C_4F_8 is used extensively in the dry etching of SiO_2, but it has a high global warming potential. [3] Thus, although this perfluorocarbon is itself a replacement for other feed-gases such as CF_4 in technological plasmas, it is important to find other alternatives which have a low global warming potential. Octafluorocyclopentene (*c*-C_5F_8) has been suggested as a potential feed-gas.[4] It is therefore surprising to find that *c*-C_5F_8 is a largely unstudied molecule, with the exception of electron attachment investigations. To our knowledge no photoionisation studies have been performed and very few reactions with ions have been reported. In this paper we report the He (I) photoelectron spectrum (PES), threshold photoelectron-photoion coincidence (TPEPICO) spectrum from 12 – 22 eV, and a study of the reactions of *c*-C_5F_8 with a range of atomic and molecular cations. To complement these studies, data from a new electron ionisation study of *c*-C_5F_8 are also reported.

There have been a number of studies investigating low energy electron attachment to *c*-C_5F_8, for which both rate coefficients and anion products have been measured.[5-7] The electron attachment occurs essentially by s-wave capture with a rate coefficient of 3.62×10^{-7} cm^3 $molecule^{-1}$ s^{-1}, and the dominant product anion is $C_5F_8^-$. The structure of *c*-C_5F_8 has been determined by electron diffraction,[8] and its multiphoton infra-red dissociation has been well documented.[9,10] To our knowledge, only two studies of the ion-molecule reactions of *c*-C_5F_8 have been published.[11,12] One study presents the kinetics and products of some cation molecule reactions using a Fourier Transform Mass Spectrometer (FTMS). In addition, the electron ionisation cross-sections for *c*-C_5F_8 from threshold to 200 eV have been measured,[11] this provides the only reported first ionisation energy at 11.6 eV. The second study investigated cation and anion molecule reactions in a high pressure environment.[12]

One aim of this work is to gain insight into how electron transfer occurs in bimolecular reactions. Two mechanisms have been postulated, defined as long-range electron transfer and short-range electron transfer.[1,13,14] Briefly, in long-range electron transfer the neutral molecule exchanges an electron with the cation at a large internuclear distance (~ 5Å). It is assumed that the cation of the neutral molecule formed is weakly influenced by the presence of the reacting cation. The neutral molecule acts, to all intents and purposes, as if it has been ionised by a resonant photon and, therefore, the product ion branching ratios from the ion-molecule and photoionisation experiments should be similar. Short-range electron transfer occurs when the electron jump happens at a much closer separation of the reacting cation and the neutral molecule, through the formation of a complex. The cation of the neutral molecule is now formed under the influence of the reacting ion, and this may lead to differences in the branching ratios for the bimolecular reaction

compared to the photon experiment. Another mechanism can occur in a collision complex where bond making and breaking may take place; our definition of a chemical reaction. For electron transfer, daughter ions can form *via* fragmentation of the parent cation of the neutral molecule. In the chemical mechanism, daughter ions are formed in the complex and not with the parent ion as an intermediate.

2. Experimental

The apparatus used for the TPEPICO study has been described in detail previously.[15] The experiments were performed at the Daresbury Synchrotron Radiation Source (SRS) on stations 3.1 and 3.2 using the 1m Wadsworth and 5 m McPherson monochromator respectively.[16,17] The synchrotron radiation is coupled into the reaction region *via* a capillary, and the flux is subsequently monitored by a photomultiplier tube using a sodium salicylate window. Threshold photoelectrons and fragment cations are extracted in opposite directions by an electric field of 20 V cm^{-1}. The electrons are detected in a threshold analyser with resolution *ca.* 10 meV, the ions in a linear time-of-flight (TOF) mass spectrometer with a resolution, $m/\Delta m$, of *ca.* 200. The signals are detected by a channeltron and a pair of microchannel plates, respectively. The raw data pulses are discriminated and pass to a time-to-digital convertor. The electrons provide a start to the TOF detection window and the ions provide a stop, allowing signals from the same ionisation event to be detected in coincidence. Spectra are measured as a function of photon energy, where the data are recorded as three-dimensional maps of coincidence count *vs.* ion TOF *vs.* photon energy. These spectra can yield either the TOF mass spectrum at any photon energy or the yield of any fragment ion as a function of energy. Extraction of product branching ratios as a function of photon energy is facile, and in addition the threshold photoelectron spectrum and total photoion cross section are recorded as part of the coincidence experiment. It is also possible to record TOF spectra at higher time resolution to yield kinetic energy releases, but these measurements were not made for this molecule.

The SIFT technique has been reviewed in detail,[18,19] and full details of the current mode of operation of the Birmingham apparatus are given elsewhere.[14] Briefly, the apparatus consists of an ion source where neutral gases are ionised under high pressure by 70 eV electron ionisation. The required ion is selected using a quadrupole mass filter before being admitted into the flow tube, where it is carried along by a flow of high purity (99.997%) helium gas at a pressure of *ca.* 0.5 Torr. The neutral reagent is then injected downstream into the flow tube *via* one of two different inlets. Any resultant ionic products are detected by a second quadrupole mass spectrometer. The amount of injected neutral is varied from zero to a value which depletes the reactant ion signal by *ca.* 90%. The loss of reagent ion and the increase in product ions are recorded as a function of neutral reagent concentration under pseudo-first-order conditions. The error in the rate coefficient determined from the analysis is estimated to be 20%, and the apparatus is limited to measuring reactions with rate coefficients greater than *ca.* 10^{-13} cm^3 $molecule^{-1}$ s^{-1}. Branching ratios are derived from

plots of ion signal *vs.* neutral concentration, and extrapolation to zero flow of the neutral molecule allows for the effects of any secondary reactions. We quote an error of 15% in product branching ratios, this error increasing for ratios below 10%.

3. Theoretical calculations

3.1 *Ab initio* calculations

To aid interpretation of the results *ab initio* calculations were performed using Gaussian 03.[20] Starting from electron diffraction data,[8] the structure of *c*-C_5F_8 was first optimised at the DFT B3LYP level with a 6-311 G + (d,p) basis set. The molecule has C_s symmetry, the geometry is puckered and not planar. The carbon atom opposite the carbon-carbon double bond is raised above the plane of the molecule by around 22°, less than in the hydrogen analogue.[8] From this optimised structure the vertical ionisation energy (VIE) was calculated using the outer valence Green's function (OVGF) method built into Gaussian 03. By definition, G03 only calculates the OVGF energies up to 20 eV. There is no experimental or *ab initio* value for the enthalpy of formation of *c*-C_5F_8 in the literature. We use a value of -1495 kJ mol^{-1}, with a conservative error of ± 20 kJ mol^{-1}. This value was calculated at the DFT B3LYP level with a 6-311 G + (d,p) basis set. The methodology was to use Gaussian 03 to generate the vibrational frequencies for *c*-C_5F_8 and a series of smaller related molecules.[21] Some examples of molecules used are CF_3, C_2F_4 and C_2F_2. Using the values for the total internal energy plus a thermal correction, which is equivalent to $\Delta_fH^0_{298}$, an enthalpy change for a series of 'reactions' in which *c*-C_5F_8 was produced were calculated. These numbers were then used with known values for Δ_fH_{298} for the molecules used to give a value for $\Delta_fH^0_{298}$[*c*-C_5F_8].

Similarly, no value was available in the literature for $\Delta_fH^0_{298}$[*c*-$C_5F_7^+$]. In principle, this number can be calculated from our TPEPICO data using the appearance energy (AE_{298}) for $C_5F_7^+$ for the reaction:

$$c\text{-}C_5F_8 \rightarrow C_5F_7^+ + F + e^- \qquad \text{(I)}$$

Using a Hess' cycle and assuming that the measured AE_{298} plus the thermal correction due to Traeger and McLoughlin [22] is identical to the thermochemical threshold, *i.e.* no kinetic shift or exit channel barrier is present, we determine the enthalpy of formation to be –84 kJ mol^{-1}. A second method to determine $\Delta_fH^0_{298}$[*c*-$C_5F_7^+$] uses the bracketed value for the fluoride ion affinity (FIA) of $C_5F_7^+$, $1001 \leq FIA(C_5F_7^+) \leq 1045$ kJ mol^{-1} (Section 5.2.1). The FIA of $C_5F_7^+$ is defined as the negative of the enthalpy of reaction for:

$$C_5F_7^+ + F^- \rightarrow c\text{-}C_5F_7 \qquad \text{(II)}$$

This method then gives $-245 \leq \Delta_fH^0_{298}(c\text{-}C_5F_7^+) \leq -201$ kJmol^{-1}. However, both these methods are dependent on the value used for $\Delta_fH^0_{298}$[*c*-C_5F_8]. To determine a value which is independent of it, we first used the *ab initio* method outlined above for *c*-C_5F_8 to obtain $\Delta_fH^0_{298}$[*c*-C_5F_7], –1105 ± 30 kJ mol^{-1}. A value for the adiabatic ionisation energy of C_5F_7 was calculated using Gaussian 03 to be 9.66 eV, yielding

$\Delta_f H^0_{298}[c\text{-}C_5F_7^+]$ to be −173 ± 50 kJ mol^{-1}. Thus there is a range of ~160 kJ mol^{-1} for the possible values of $\Delta_f H^0_{298}(c\text{-}C_5F_7^+)$. Due to the closeness in values between that using the Gaussian calculation of the enthalpy of formation and that using the FIA method, we have chosen to use a value of –223 kJ mol^{-1} in tables 1 and 2, which is the mid-point of the range determined by the FIA method. This method is also likely to have the least error associated with it.

3.2 Calculation of reaction rate coefficients

For each ion-molecule reaction studied a theoretical rate coefficient (k_{th}) was calculated for comparison to the experimental value (k_{exp}). This rate coefficient was calculated using the Modified Averaged Dipole Orientation (MADO) theory,[23-25] this method being based on the classical collisional model of Langevin.[26] The calculation requires values for the polarisability volume (α') and the dipole moment (μ) of the neutral reactant and the reduced mass of the collision partners. Neither α' or μ have been measured for c-C_5F_8, so α' was estimated using the method of Miller.[27] This procedure uses atomic hybrid components to estimate the molecular polarisability volume in an additive fashion, giving a value of 9.38×10^{-30} m^3. The value of μ was taken from the DFT Gaussian 03 calculations, 1.87 D, to be compared with a value of 2.42 D for Z-1,2-difluoroethene,[28] which has a similar configuration of atoms around the C=C bond. The ratio k_{exp} / k_{th} should not be greater than unity as this would represent the physical impossibility of a larger number of reactions than collisions between molecules. A value greater than unity for a large number of reactions could indicate that another ion-molecule interaction, other than the ion-dipole potential, needs to be considered.[1,29]

4. Energetics

Table 1 shows the energetics for the dissociative ionisation channels of c-C_5F_8. The appearance energy (AE_{298}) of an ion is taken to be the first onset of signal above the background noise. Using the method of Traeger and McLoughlin,[22] the AE_{298} value can be converted into an upper limit for the enthalpy change of the appropriate unimolecular reaction ($\Delta_r H^0_{298}$). There are several caveats to the use of this procedure. Firstly, it was developed for interpretation of photoionisation rather than TPEPICO ion yields, and the latter are the differential of the photoionisation spectrum. Secondly, the procedure is only strictly applicable for photodissociation reactions where a single bond is cleaved. With these caveats, the procedure was applied to convert AE_{298} to $\Delta_r H^0_{298}$ values for the two fragments ions formed from c-C_5F_8, as we believe it introduces more error to assume that $AE_{298} = \Delta_r H^0_{298}$ which effectively neglects thermal effects. Enthalpies of formation at 298 K were taken from the standard sources,[30,31] apart from CF_3 (–466 kJ mol^{-1}) and CF_3^+ (406 kJ mol^{-1}),[32] and c-$C_4F_6^+$ (76 kJ mol^{-1}).[33] Other values used for the calculation of thermochemistry for the SIFT data are indicated in table 2. Our method of calculation for the enthalpy of formation of c-C_5F_8, –1495

kJ mol^{-1}, is outlined in section 3.1. $\Delta_f H^0_{298}[C_5F_8^+]$ is –411 kJ mol^{-1}, this value being $\Delta_f H^0_{298}[c\text{-}C_5F_8]$ plus the IE. For this latter value we use 11.24 eV determined with electron ionisation spectroscopy by Feil *et al.*[34]

5. Results and Discussions

5.1 Results from the TPEPICO study

5.1.1 Threshold photoelectron spectrum and total relative photoion yield

Figure 1 shows the threshold photoelectron spectrum (TPES) for *c*-C_5F_8 recorded from 12.2–22.0 eV with a resolution of 0.2 nm on beamline 3.2 at the SRS. The onset of ionisation was determined to be 12.25 ± 0.05 eV. Due to second-order effects and low flux on this beamline for $\lambda > 105$ nm, scans could not be recorded below 11.8 eV. However, in a survey scan from 11.8–12.2 eV no signal is observed above the background. To our knowledge there has only been one previous experimental measurement of the IE of *c*-C_5F_8 and one *ab initio* calculation. From an electron ionisation study Jiao *et al.*[11] determined the IE to be 11.6 ± 0.7 eV, while Hiraoka *et al.*[12] calculated the IE to be 11.2 eV using B3LYP methods. To verify these values, we have performed a new electron ionisation study at the Institut für Ionenphysik in Innsbruck,[34] and a He(I) photoelectron spectrum has been recorded at the University of Southampton. The electron ionisation and photoelectron spectrometers have been described in detail elsewhere.[35,36] From these studies, the IE of *c*-C_5F_8 from electron ionisation was found to be 11.24 ± 0.10 eV, and from He(I) photoionisation to be 11.30 ± 0.05 eV (for the v=0 peak). The weak peaks below 11 eV in the He (I) spectrum (Figure 1) are most likely due to hot bands. From 11–12 eV the He (I) spectrum shows a band with clearly-resolved vibrational structure which is completely absent from the threshold spectrum. Unfortunately, due to the experimental limitations described above, TPEPICO scans were not performed below 11.8 eV under threshold conditions. However, there is a noticeable absence of signal at 11.8 eV which is approximately the centre of the ground ionic state determined in the PES measurements.

To confirm whether this conclusion is correct, a TPES was recorded independently at the Daresbury SRS. We used the penetration-field spectrometer of King which combines very high resolution (up to 0.002 eV) with excellent sensitivity.[37] The spectrum recorded at a resolution of 0.005 nm is shown in Figure 2, together with the threshold spectrum extracted from the coincidence experiment at a resolution of 0.2 nm. We have scaled the relative intensities of the two spectra such that the peak at ~13 eV has comparable intensity. Two points are apparent. First, the ground-state photoelectron band *is* observed under the enhanced sensitivity conditions of the penetrating-field spectrometer, but its intensity is indeed very weak. We determine the adiabatic IE of *c*-C_5F_8 to be 11.237 ± 0.002 eV. We conclude that the sensitivity of the threshold analyser in the coincidence apparatus is not sufficient to observe this very weak band, but we note that this apparatus is a compromise for efficient detection of both threshold electrons and mass-selected

ions.[15] Second, as both spectra are recorded nominally under threshold conditions, the relative intensities of all peaks should be similar. In practice, the relative intensity of the bands from 15 – 18 eV are significantly higher in the TPEPICO experiment. There are also many more autoionising peaks in this region recorded by the coincidence spectrometer (see later). We conclude that the threshold analyser of the coincidence spectrometer has a greater high-energy electron tail than the penetrating-field analyser. The small partial ionisation cross-section into the ground state of *c*-$C_5F_8^+$ under threshold conditions may be explained by fluorescence from, or predissociation of the initially-excited Rydberg state(s) into neutral fragments. The vibrational spacing of this band in the He (I) spectrum has an average spacing of 0.20 eV (1613 cm^{-1}) which is probably the C=C stretch. We note that the C=C stretching frequency of ethene is 1623 cm^{-1}.[38]

From our Gaussian 03 calculations the valence orbitals in C_s symmetry can be labelled as ...(11a") (19a') (20a') (12a") (13a") (21a') (22a') (14a") (15a") (23a') (24a") (16a") (17a") (25a') (18a") (26a') (27a') (19a") (28a') (20a") (29a') (21a") (30a'), where the numbering includes the core orbitals. The highest occupied molecular orbital has a' symmetry and is made up of the C=C bond π orbitals, an assignment which is confirmed by the vibrational spacing of the first band in the He (I) spectrum. The lower-energy orbitals are combinations of C-F and C-C bonds with no clear localization of electron density into a single bond, as might be expected in such a large molecule. Figure 3(a) shows the TPES of *c*-C_5F_8 recorded on beamline 3.2 at a resolution of 0.2 nm. The positions of the OVGF IE values are indicated by red drop lines. The agreement with experiment is poor. At higher energies the OVGF predictions are significantly higher in energy than peaks in the measured TPES. This is surprising because the agreement between equivalent data in *c*-C_4F_8 is excellent.[1] It is interesting that the OVGF calculations do not show the presence of the missing electronic state shown in the He(I) PES. We note that a shift of ~2 eV to lower energy in all the OVGF calculations would produce a much better agreement with the photoionisation results; this could be coincidental or significant.

In figure 3(a) there are several sharp peaks in the TPES between 16 and18 eV. Peaks at the same energies are also observed in the total relative photoion yield, although the relative intensities are sometimes different. It is most likely that these peaks arise due to autoionisation, indicated by resonances superimposed on non-resonant step functions.[39] Further evidence for autoionisation is that these resolved peaks are not present under He(I) conditions (Figure 1), whilst they are present in reduced numbers under much higher-resolution threshold electron conditions (Figure 2). Figure 4 shows the total relative photoion yield recorded from onset to 22 eV, with the insert highlighting the autoionising features from 15.5–17.0 eV. The peaks probably represent several overlapping vibrational progressions in Rydberg states.

5.1.2 Scanning threshold photoelectron-photoion coincidence spectrum

The scanning energy TPEPICO spectrum was recorded from 12-22 eV on beamline 3.1 with an optical resolution of 0.3 nm and a TOF resolution of 128 ns. Three different ions, $C_5F_8^+$, $C_5F_7^+$ and $C_4F_6^+$ were observed (figure 3(b)), and their appearance energies are listed in table 1. The first product observed is the parent ion, $C_5F_8^+$, at 12.25 ± 0.05 eV. This is the major ion up to around 13.5 eV, before the signal drops to essentially zero at 15 eV. Above 18 eV the parent ion signal rises above zero for an energy range of *ca* 4 eV before returning to zero at 22 eV. The first fragment ion formed is $C_4F_6^+$ with an AE_{298} of 12.73 ± 0.05 eV which dominates till ~15 eV. The second and final fragment ion formed is $C_5F_7^+$ with an AE_{298} value of 15.14 ± 0.15 eV. It should be noted that some structure occurs in the $C_5F_7^+$ signal below this energy. However, as this onset is sharp, it is felt that these lower-energy features between 13 and 15 eV are probably artefacts of the analysis from the background subtraction technique which has been used. Above 18 eV all three ions form with roughly equal percentage.

It is interesting to note that formation of $C_4F_6^+$, involving the breaking of two C-C bonds, has a lower appearance energy than formation of $C_5F_7^+$,where only a single C-F bond is broken, and this fact has been noted for other fluorocarbons by Bauschlicher and Ricca.[33] Jiao *et al*. saw the same ordering of appearance energies for $C_5F_8^+$, $C_5F_7^+$ and $C_4F_6^+$ following electron ionisation of *c*-C_5F_8.[11] They also observed $C_4F_5^+$, $C_3F_3^+$, $C_3F_4^+$, CF^+ and CF_2^+ as products. Their appearance energies, however, for $C_4F_6^+$ and $C_5F_7^+$, 14.2 and 17.5 eV, are significantly higher than our values. An obvious explanation for such differences is that their work was carried out in a FTMS where ions are trapped for an appreciable length of time. Such long storage times could lead to further fragmentation of product ions if they are metastable, giving rise to the extra fragments which we do not observe. We note that the recent electron ionisation study performed by Feil *et al*,[34] whilst observing the same range of ions as detected in the FTMS experiment, gives similar appearance energies for $C_4F_6^+$ and $C_5F_7^+$ to our coincidence study.

In table 1 the measured appearance energies have been converted into $\Delta_r H^0_{298}$ values using the method of Traeger and McLoughlin.[22] This method was applied to formation of $C_4F_6^+$, although it is an approximation for the reasons outlined in section 4, and $C_5F_7^+$. These experimental values were compared to the thermochemical values. For $C_4F_6^+$ the experimental value is actually below the thermochemical value. The difference is around 27 kJ mol^{-1}, and undoubtedly arises due to uncertainty in the calculated enthalpy of formation of *c*-C_5F_8 and our application of the Traeger and McLoughlin method. However, within reasonable error limits, it seems that the $C_4F_6^+$ onset cannot be associated with formation of *cyclic*-$C_4F_6^+$ but must involve formation of *linear*-$C_4F_6^+$. This is in agreement with the retro Diels-Alder mechanism suggested by Jiao *et al.* for formation of *linear*-$C_4F_6^+$.[11] The calculated enthalpy of reaction for $C_5F_7^+ + F$ lies 1.44 eV below the experimental value. For such a simple C-F bond cleavage, an exit-channel barrier of this magnitude is very unlikely. The lack of agreement may reflect on the *ab initio* values used for the enthalpy of formation of both *c*-C_5F_8 and $C_5F_7^+$.

5.2 Selected Ion Flow Tube Results

5.2.1 Rate coefficients

The reactions of *c*-C_5F_8 with twenty two atomic and molecular reactant ions have been studied using the SIFT apparatus. The ions had a range of recombination energies (RE) from 6.27 – 21.56 eV. Five ions did not react; H_3O^+, SF_3^+ NO^+, SF_5^+ and SF_2^+. The fact that H_3O^+ did not react by proton transfer shows that the proton affinity of *c*-C_5F_8 is less than that of H_2O, *i.e.* < 691 kJ mol^{-1}. Comparisons can be made between the calculated MADO rate coefficient and the experimentally measured rate coefficient to determine the efficiency of the reaction (see table 2). To calculate the MADO value the dipole moment of *c*-C_5F_8 is needed. Unfortunately this value has never been measured, and we used a value of 1.87 D from our Gaussian 03 *ab initio* calculations. There is excellent agreement between experimental and theoretical rate coefficients, suggesting that our values for μ and α' are reasonable.

Most of the reactions go at or near (within 30%) of the collisional rate, and so are very efficient. However, there are two slow reactions. The slowest is the reaction of SF^+ with *c*-C_5F_8 which is only 10% efficient. There is unlikely to be significant steric hindrance for such a reaction and the disagreement is most likely because the reaction is slightly endothermic. The absence of reaction of SF_3^+, SF_5^+ or SF_2^+ with *c*-C_5F_8 can then allow the fluoride ion affinity, FIA, of $C_5F_7^+$ to be bracketed between that of SF_5^+ and SF^+, ***i.e.*** 1001 ≤ FIA($C_5F_7^+$) ≤ 1045 kJ mol^{-1}.[40] As there is a slow reaction with SF^+ but not with SF_5^+, the data suggests that the FIA($C_5F_7^+$) may lie closer to the FIA(SF^+) value. The second slow reaction is H_2O^+ + *c*-C_5F_8 which reacts with 55% efficiency. The main product is *c*-$C_5F_8^+$. We note that N_2O^+, with a similar RE to H_2O^+, reacts with *c*-C_5F_8 at the collisional rate. We suggest that H_2O^+ does not react with *c*-C_5F_8 *via* long range charge transfer, but *via* a shorter range mechanism where steric effects may be important.

5.2.2 Branching Ratios

Table 2 shows the experimental and MADO rate coefficients (Column 2), the MADO values being given in square brackets, and the ionic products and branching ratios (Column 3) for the reactions of *c*-C_5F_8 with the cations used in this study. Proposed neutral products based on mass conservation and thermodynamics are in column 4 and column 5 lists corresponding enthalpies of reactions. The pathways shown are those which are both the most exothermic and chemically feasible. In cases where there is more than one possible pathway an indicative selection is presented.

Eight ions whose RE falls below 11.24 eV were studied. Five ions did not react. The remaining three, CF_3^+, CF^+ and SF^+ react by fluoride abstraction to form $C_5F_7^+$ as the ionic product. The TPEPICO experiment shows that when fragmentation is initiated by a photon it is more facile to break C-C σ-bonds

than C-F σ-bonds. However, the reactions with these three ions break the C-F bond. This shows the differences that can occur when reactions are initiated chemically, rather than by photons. CF_2^+ has an RE of 11.44 eV and so non-dissociative electron transfer is possible, instead only a F^- abstraction channel occurs to form $C_5F_7^+$. The dominant ion as a result of ion-molecule reactions with ions with RE from 11.24 eV to 13.5 eV is $C_5F_8^+$. For higher RE, $C_4F_6^+$ becomes as strong as the parent ion until ~15 eV when $C_5F_7^+$ is the major ion. From ~ 17 eV upwards the branching ratio to $C_3F_3^+$ becomes significant, and for Ne^+ (RE = 21.56 eV) it is the major product ion.

There are only two other studies of the ion-molecule reactions of *c*-C_5F_8 with which to compare our results; the work of Jiao *et al* using a FTMS and of Hiraoka *et al* using an electron mass spectrometer.[11,12] The work of Hiraoka *et al* largely concentrates on negative ions and cluster formation. The only comparable reaction is *c*-$C_5F_8 + N_2^+$. Parent ion is the only product, while in the SIFT experiment three daughter ions are detected of which the parent is only a minor channel. However, the experiment of Hiraoka *et al.* is performed at higher pressures (several Torr). Furthermore the reactant ions are formed by a 2kV electron pulse and could be either N_2^+ or $N_2 \cdot N_2^+$. If N_2^+ is the reactant ion then the lack of products other than $C_5F_8^+$ could be due to collisional stabilisation at the high pressures used. The work of Jiao *et al.*[11] contains three reactions with which we can make comparisons; those of CF_3^+, CF^+ and Ar^+. For the reactions of CF_3^+ and CF^+, our SIFT results agree with the FTMS results, the only ionic product being $C_5F_7^+$. For Ar^+ there are some differences in branching ratios, but only of the minor channels. For example $C_5F_8^+$ is detected at the 5 % level in the SIFT and $C_3F_3^+$ is not detected, whereas this situation is reversed in the FTMS study. Such differences are most likely due to the extremely low pressure in a FTMS and hence absence of collisional stabilisation of metastable ions. This can lead to more fragmentation in comparison to a higher-pressure experiment such as the SIFT. We note that Jiao *et al.* are only able to quote rates for the three reactions relative to that measured for the Ar^+ reaction. Our absolute values do not agree with these relative values. The difference could be due to uncertainties in the translational energy of ions in a FTMS.

We comment that many of the channels forming $C_5F_7^+$ and $C_4F_6^+$ with significant branching ratios are calculated to be endothermic. We are using one of the most negative values for $\Delta_f H^0_{298}[C_5F_7^+]$, –223 kJ mol^{-1}, of all the possible values described in section 3.1. The experimental value, –84 kJ mol^{-1}, leads to an even higher endothermicity for all reactions forming $C_5F_7^+$. Interpretations of reactions forming $C_4F_6^+$ are hindered by the lack of knowledge of the isomer formed, whether it is linear or cyclic, although we note that the values of table 2 assume the linear form is produced. We believe that the apparent endothermicities of such reactions arise from the accumulation of errors for $\Delta_f H^0_{298}$ values of *c*-C_5F_8, $C_5F_7^+$ and linear-$C_4F_6^+$.

6. Comparison of TPEPICO and SIFT branching ratios

Figure 3(c) shows the branching ratios from the TPEPICO and SIFT studies as a function of energy. The former appear as continuous graphs, whereas the latter appear as data points at the defined RE value of each ion. Only fragment ions from the SIFT study which are also observed in the TPEPICO experiment are indicated. A comparison of the branching ratios may indicate which mechanism is occurring in the ion-molecule reactions. If the branching ratios are similar to those from photon ionisation, long-range charge transfer may be dominant; if they are different, short-range charge transfer or a chemical reaction is probably occurring. Agreement between the two experiments is good in the range 12–13 eV which covers the Franck-Condon envelope of the $\widetilde{A}$ state of $C_5F_8^+$. The only anomalous ion in this range is H_2O^+ which, as stated earlier, reacts with low efficiency. This is further evidence that H_2O^+ may not react by long-range charge transfer, but instead forms a tight collision complex where steric effects and orientation will be important and inhibit the reaction channel. Other ions in this energy range probably react *via* long-range charge transfer. For energies in the range 13–17 eV the agreement is slightly less satisfactory between TPEPICO and SIFT results. Both experiments, however, show the same trends for the fragment ions. Therefore, it seems likely that a long-range mechanism, not a short-range mechanism, operates for ions in this range. The only ion which shows a significant variation from the TPEPICO branching ratios is N^+ (RE = 14.53 eV), as observed in previous work.[1,14] It appears that reaction with N^+ causes much 'softer' ionisation (*i.e.* less fragmentation) than expected for a cation with this RE value. One explanation may be that some fraction of the N product is formed as N* (^{2}D) with an internal energy of 2.38 eV. Less energy would then be available for ionisation and subsequent fragmentation of *c*-C_5F_8. For F^+ (RE = 17.42 eV), the agreement between the branching ratios is much better, within the 15% error we define as indicating agreement.[41] For Ne^+ (RE = 21.56 eV), however, there is poor agreement, and many more fragments are formed than from photoionisation at this energy. For this ion, therefore, it is likely that a compact collision complex is forming and reaction proceeds by a short range process.

7. Conclusions

The threshold photoelectron, the threshold photoelectron photoion coincidence spectrum, and the total ion yield have been recorded for *c*-C_5F_8 from 12–22 eV. Detection of an ion signal from our TPEPICO measurements for *c*-C_5F_8 occurred at 12.25 eV, which corresponds to the first excited electronic state of the parent ion, *i.e.* the ground state is undetectable in our TPEPICO measurements. The energy-selected ion yields of the three product ions, $C_5F_8^+$, $C_5F_7^+$ and $C_4F_6^+$, from 12–22 eV have been measured. A He (I) photoelectron spectrum has been recorded and gives the first adiabatic ionisation energy for *c*-C_5F_8 to be 11.30 eV. A high resolution electron ionisation study has also been performed, yielding a first ionisation

energy of 11.24 eV. A much higher-resolution TPES has also been performed which shows that the ground ionic state is present but only with very low intensity; the adiabatic IE is 11.237 eV.

Branching ratios and rate coefficients at 298 K for the reaction of twenty two cations with *c*-C_5F_8 have been recorded in a selected ion flow tube. Most of the ions studied react with high efficiency. The absence of reaction between H_3O^+ and *c*-C_5F_8 has allowed an upper limit to be placed on the proton affinity *c*-C_5F_8. Similarly, the fluoride abstraction reactions with SF_x^+ (x = 1–5) and CF_n^+ (n = 1–3) have allowed upper and lower limits to be placed on the fluoride ion affinity of *c*-C_5F_8. Comparison with TPEPICO data suggests that the majority of ions react *via* a long-range charge transfer mechanism. N^+ behaves in this, as in several previous studies[1,14] as a 'soft' chemical ioniser. One explanation may be that some of the product N atoms are formed electronically excited, leading to less internal energy being available to fragment $C_5F_8^+$. Using Gaussian 03 the enthalpy of formation of *c*-C_5F_8 has been calculated to be –1495 kJ mol^{-1}.

The most interesting result in this comprehensive study of the formation of positive ions from *c*-C_5F_8 is found in the photoionisation data. The first photoelectron band, which is clearly visible in the He(I) spectrum with vibrationally-resolved structure, is almost completely absent from the threshold photoelectron spectrum. This result may be due to either fluorescence from or predissociation of the Rydberg state into neutrals, rather than ionisation. It is well known that different vibrational distributions of a molecular photoelectron band can be observed under resonant and non-resonant conditions. However, to our knowledge, this is a very rare example of a molecular photoelectron spectrum showing a band under one set of ionisation (*i.e.* non-resonant) conditions, whilst being almost completely absent under different (*i.e.* resonant or threshold) conditions.

Acknowledgments

We are grateful to EPRSC for grants (GR/S21557 and GR/M42974), and for the Daresbury staff, especially Drs David Shaw and Andrew Malins. We also thank Matthew Simpson for extensive assistance during these experiments. We are especially grateful to Dr Jeremy Harvey (University of Bristol) for advice on the calculation of the enthalpy of formation for *c*-C_5F_8 and C_5F_7. CAM thanks ESF (EIPAM network) for short visit grant 789 and the University of Innsbruck for the hospitality shown. MAP thanks Professor John Dyke (University of Southampton) for assistance in running the He (I) photoelectron spectrum of *c*-C_5F_8, and Professor George King (University of Manchester) and Dr. Michele Siggel-King (Daresbury Laboratory) for assistance in acquiring its very high-resolution threshold photoelectron spectrum. MAP and SA both thank the University of Birmingham for studentships.

References

1 M.A. Parkes, S. Ali, R.P. Tuckett, V.A. Mikhailov and C.A. Mayhew, *Phys. Chem. Chem. Phys.*, 2006, **8,** 3643.

2 C.A. Mayhew, A.D.J. Critchley, D.C. Howse, V. Mikhailov and M.A. Parkes, *Euro. Phys. J. D*, 2005, **35,** 307.

3 L.G. Christophorou and J.K. Olthoff: *Fundamental Electron Interactions with Plasma Processing Gases*, Kluwer Academic / Plenum Publishers, New York, 2004.

4 M. Ooka and S. Yokoyama, *Jpn. J. Appl. Phys.*, 2005, **44,** 6476.

5 R.Y. Pai, L.G. Christophorou and A.A. Christodoulides, *J. Chem. Phys.*, 1979, **70,** 1169.

6 A. Chutjian and S.H. Alajajian, *J. Phys. B*, 1985, **18,** 4159.

7 B.G. Zollars, K.A. Smith and F.B. Dunning, *J. Chem. Phys.*, 1984, **81,** 3158.

8 C.-H. Chang and S.H. Bauer, *J. Phys. Chem.*, 1971, **75,** 1685.

9 P.K. Chowdhury, *J. Phys. Chem*, 1995, **99,** 12084.

10 P.K. Chowdhury, K.V.S.R. Rao and J.P. Mittal, *J. Phys. Chem.*, 1986, **90,** 2877.

11 C.Q. Jiao, C.A. De Joseph, Jr. and A. Garscadden, *J. Phys. D*, 2005, **38,** 1076.

12 K. Hiraoka, K. Fujita, M. Ishida, T. Ichikawa, H. Okada, K. Hiizumi, A. Wada, K. Takao, S. Yamabe and N. Tsuchida, *J. Phys. Chem. A*, 2005, **109,** 1049.

13 G.K. Jarvis, R.A. Kennedy, C.A. Mayhew and R.P. Tuckett, *Int. J. Mass Spec.*, 2000, **202,** 323.

14 V.A. Mikhailov, M.A. Parkes, R.P. Tuckett and C.A. Mayhew, *J. Phys. Chem. A*, 2006, **110,** 5760.

15 P.A. Hatherly, D.M. Smith and R.P. Tuckett, *Zeit. Phys. Chem.*, 1996, **195,** 97.

16 C.R. Howle, S. Ali, R.P. Tuckett, D.A. Shaw and J.B. West, *Nucl. Instru. Meth. B*, 2005, **237,** 656.

17 D.M.P. Holland, J.B. West, A.A. Macdowell, I.H. Munro and A.G. Beckett, *Nucl. Instrum. Meth. B*, 1989, **44,** 233.

18 D. Smith and N.A. Adams, *Adv. Atom. Mol. Phys.*, 1988, **24,** 1.

19 D.K. Böhme, *Int. J. Mass Spec.*, 2000, **200,** 97.

20 Gaussian 3, *Revision C.02*, M.J. Frisch, G.W. Trucks, H.B. Schlegel, G.E. Scuseria, M.A. Robb, J.R. Cheeseman, J.A.M. Jr., T. Vreven, K.N. Kudin, J.C. Burant, J.M. Millam, S.S. Iyengar, J. Tomasi, V. Barone, B. Mennucci, M. Cossi, G. Scalmani, N. Rega, G.A. Petersson, H. Nakatsuji, M. Hada, M. Ehara, K. Toyota, R. Fukuda, J. Hasegawa, M. Ishida, T. Nakajima, Y. Honda, O. Kitao, H. Nakai, M. Klene, X. Li, J. E. Knox, H. P. Hratchian, J. B. Cross, V. Bakken, C. Adamo, J. Jaramillo, R. Gomperts, R. E. Stratmann, O. Yazyev, A. J. Austin, R. Cammi, C. Pomelli, J. W. Ochterski, P. Y. Ayala, K. Morokuma, G. A. Voth, P. Salvador, J. J. Dannenberg, V. G. Zakrzewski, S. Dapprich, A. D. Daniels, M. C. Strain, O. Farkas, D. K. Malick, A. D. Rabuck, K. Raghavachari, J. B. Foresman, J. V. Ortiz, Q. Cui, A. G. Baboul, S. Clifford, J. Cioslowski, B. B. Stefanov, G. Liu, A. Liashenko, P. Piskorz, I. Komaromi, R. L. Martin, D. J. Fox, T. Keith, M. A. Al-Laham, C. Y. Peng, A. Nanayakkara, M. Challacombe, P. M. W. Gill, B. Johnson, M. W. Chen, W. Wong, C. Gonzalez and J.A. Pople, Gaussian Inc., Wallingford CT, 2004

21 J.N. Harvey, *Private Communication*.

22 J.C. Traeger and R.G. McLoughlin, *J. Am. Chem. Soc.*, 1981, **103,** 3647.

23 T. Su, *J. Chem. Phys.*, 1988, **88,** 4102.

24 T. Su, *J. Chem. Phys.*, 1988, **89,** 5355.

25 T. Su and W.J. Chesnavich, *J. Chem. Phys.*, 1982, **76,** 5183.

26 P.M. Langevin, *Ann. Chim. Phys.*, 1905, **5,** 245.

27 K.J. Miller, *J. A. Chem. Soc.*, 1990, **112,** 8533.

28 V.W. Laurie, *J. Chem. Phys.*, 1961, **34,** 291.

29 P.K. Bhowmik and T. Su, *J. Chem. Phys.*, 1991, **94,** 6444.

30 M.W. Chase, *J. Phys. Chem. Ref. Data*, 1998, Monograph no. 9.

31 S.G. Lias, J.E. Bartmess, J.F. Liebman, J.L. Holmes, R.D. Levin and W.G. Mallard, *J. Phys. Chem. Ref. Data*, 1988, **17,** supplement no 1.
32 G.A. Garcia, P.-M. Guyon and I. Powis, *J. Phys. Chem. A*, 2001, **105,** 8296.
33 C.W. Bauschlicher and A. Ricca, *J. Phys. Chem. A*, 2000, **104,** 9026.
34 S. Feil, P. Scheier, T.D. Märk and C.A. Mayhew, *Unpublished Data*.
35 V. Grill, H. Drexel, W. Sailer, M. Lezius and T.D. Märk, *Int. J. Mass Spec.*, 2001, **205,** 209.
36 J.M. Dyke, A. Morris and N. Jonathon, *Int. Rev. Phys. Chem.*, 1982, **2,** 3.
37 R.I. Hall, A. McConkey, K. Ellis, G. Dawber, L. Avaldi, M.A. Macdonald and G.C. King, *Meas. Sci. Tech.*, 1992, **3**, 316.
38 T. Shimanouchi: *Tables of Molecular Vibrational Frequencies Consolidated Volume I*, National Bureau of Standards, 1972.
39 G.K. Jarvis, K.J. Boyle, C.A. Mayhew and R.P. Tuckett, *J. Phys. Chem. A*, 1998, **102,** 3219.
40 M. O'Keeffe, *J. Am. Chem. Soc.*, 1986, **108,** 434`.
41 M.A. Parkes, R.Y.L. Chim, C.A. Mayhew, V.A. Mikhailov and R.P. Tuckett, *Mol. Phys.*, 2006, **104,** 263.
42 C.W. Bauschlicher and A. Ricca, *J. Phys. Chem.*, 1998, **102,** 4722.
43 C.W. Bauschlicher and A. Ricca, *J. Phys. Chem. A*, 2000, **104,** 4581.

Table 1. Thermochemistry of the observed dissociative ionisation pathways of *c*-C_5F_8 at 298 K.

	AE_{298} [a] / eV	$\Delta_r H^o_{298,exp}$ [b] / eV	$\Delta_r H^o_{298,calc}$ [c] / eV
Major Products of *c*-C_5F_8 (−1495) [d,e,f]			
c-$C_5F_8^+$(−411) [f] + e^-	12.25 [g]	-	-
$C_5F_7^+$(−223) [h] + F(+79)	15.14	15.44	14.00
Minor Products of *c*-C_5F_8 [i]			
$C_4F_6^+$(−21) + CF_2 (−182) + e^-	12.73	13.11 [j]	13.39
c-$C_4F_6^+$(+76) + CF_2 (−182) + e^-	12.73	13.11 [j]	14.39

[a] Experimentally derived appearance energies, measured from onset of signal above noise.

[b] Experimentally measured enthalpy of unimolecular reaction, derived using the method of Traeger and McLoughlin.[22]

[c] Calculated value for $\Delta_r H^o_{298,calc}$ given by literature values of $\Delta_f H^o_{298}$(products) − $\Delta_f H^o_{298}$(reactants).

[d] Major products are either the parent ion or fragments caused by breaking of a single bond.

[e] Literature values for $\Delta_f H^o_{298}$ are given in kJ mol^{-1} in brackets in column 1.

[f] Calculated using *ab initio* methods, see text.

[g] From TPEPICO spectroscopy. Electron ionisation and ultra-high sensitivity photoelectron spectroscopy determine significantly lower values of 11.24 ± 0.10 and 11.237 ± 0.002 eV, respectively (see text).[34]

[h] Calculated from the fluoride affinity of $C_5F_7^+$, see Section 3.1.

[i] Minor products are fragments formed by breaking of more than one bond.

[j] Approximate value as more than one bond is broken during dissociation

Table 2. Rate coefficients at 298 K, product cations and branching ratios, and suggested neutral products for reactions of gas-phase cations with *c*-C_5F_8. The second column shows experimental rate coefficients, with the MADO calculated values being given in square brackets. The calculated enthalpy of reaction at 298 K is shown in the fifth column.[a] The dashed line represents the position of the onset of ionisation of *c*-C_5F_8 measured by electron ionisation.

Reagent ion (RE [b] / eV)	Rate coefficient / 10^{-9} cm^3 molecule^{-1} s^{-1}	Product ions (%)	Proposed neutral products	$\Delta_r H^o_{298}$ / kJ mol^{-1}
H_3O^+ (6.27)	- [2.8]	No Reaction [c]	-	-
SF_3^+ (8.32)	- [1.5]	No Reaction	-	-
CF_3^+ (9.04)	1.2 [1.6]	$C_5F_7^+$ (100)	CF_4	-66
CF^+ (9.11)	2.0 [2.3]	$C_5F_7^+$ (100)	CF_2	-43
NO^+ (9.26)	- [2.3]	No Reaction	-	-
SF_5^+ (9.78)	- [1.3]	No Reaction	-	-
SF_2^+ (10.24)	- [1.6]	No Reaction	-	-
SF^+ (10.31)	0.2 [1.8]	$C_5F_7^+$ (100)	SF_2	-21
CF_2^+ (11.44)	2.0 [1.9]	$C_5F_7^+$ (100)	CF_3	-115
O_2^+ (12.07)	2.4 [2.2]	$C_5F_8^+$ (100)	O_2	-80
Xe^+ (12.13/13.44)	1.3 [1.3]	$C_5F_8^+$ (88) $C_4F_6^+$ [e] (12)	Xe Xe + CF_2	-86 +122
H_2O^+ (12.62)	1.6 [2.9]	$C_5F_8^+$ (66) $C_5F_7^+$ (27) $C_4F_6^+$ (7)	H_2O H_2O + F HF + OH CF_2 + H_2O	-132 +136 +65 +75
N_2O^+ (12.89)	2.1 [1.9]	$C_5F_8^+$ (85) $C_5F_7^+$ (1)	N_2O N_2O + F N_2 + OF	-159 +109 +56

		$C_4F_6^+$ (14)	$N_2O + CF_2$	+48
			$OCF_2 + N_2$	-491
O^+	2.6	Not Recorded	-	-
(13.62)	[3.0]			
CO_2^+	2.0	$C_5F_8^+$ (42)	CO_2	-244
(13.76)	[2.0]	$C_5F_7^+$ (4)	$CO_2 + F$	+24
			CO_2F	-18
		$C_4F_6^+$ (50)	$CO_2 + CF_2$	-37
			$CO + OCF_2$	-210
		$C_4F_5^+$ [f](4)	$CO_2 + CF_3$	-114
Kr^+	1.6	$C_5F_8^+$ (23)	Kr	-266
(14.00)	[1.5]	$C_5F_7^+$ (1)	Kr + F	+2
		$C_4F_6^+$ (70)	$Kr + CF_2$	-59
		$C_4F_5^+$ (6)	$Kr + CF_3$	-136
CO^+	2.4	$C_5F_8^+$ (31)	CO	-267
(14.01)	[2.4]	$C_5F_7^+$ (5)	CO + F	+1
			COF	-143
		$C_4F_6^+$ (60)	$CO + CF_2$	-60
		$C_4F_5^+$ (4)	$CO + CF_3$	-137
N^+	2.5	$C_5F_8^+$ (38)	N	-318
(14.53)	[3.3]	$C_5F_7^+$ (8)	N + F	-50
			NF	-354
		$C_4F_6^+$ (47)	$N + CF_2$	-110
			FCN + F	-286
		$C_4F_5^+$ (5)	$N + CF_3$	-188
		$C_3F_3^+$ (2)	$N + C_2F_5$	-800 - $\Delta_f H^o_{298}[C_3F_3^+]$
			$CF_3CN + F_2$	-875 - $\Delta_f H^o_{298}[C_3F_3^+]$
N_2^+	1.9	$C_5F_8^+$ (9)	N_2	-419
(15.58)	[2.4]	$C_5F_7^+$ (47)	$N_2 + F$	-151
		$C_4F_6^+$ (44)	$CF_2 + N_2$	-211
Ar^+	1.9	$C_5F_8^+$ (5)	Ar	-437
(15.76)	[1.6]	$C_5F_7^+$ (54)	Ar + F	-169
		$C_4F_6^+$ (38)	$Ar + CF_2$	-229
		$C_4F_5^+$ (3)	$Ar + CF_3$	-307
F^+	2.9	$C_5F_8^+$ (3)	F	-596
(17.42)	[2.8]	$C_5F_7^+$ (47)	F + F	-279
			F_2	-487
		$C_4F_6^+$ (23)	$F + CF_2$	-389
			CF_3	-752
		$C_4F_5^+$ (6)	$F + CF_4$	-466
			CF_4	-1013
		$C_3F_3^+$ (21)	$F + C_2F_5$	-1079 - $\Delta_f H^o_{298}[C_3F_3^+]$
			C_2F_6	-1609 - $\Delta_f H^o_{298}[C_3F_3^+]$
Ne^+	2.2	$C_5F_8^+$ (7)	Ne	-996
(21.56)	[2.7]	$C_5F_7^+$ (3)	Ne + F	-728
		$C_5F_6^+$ (2)	$Ne + F_2$	-585 - $\Delta_f H^o_{298}[C_5F_6^+]$

$C_4F_6^+$ (2)	Ne + CF_2	-788
$C_4F_5^+$ (15)	Ne + CF_3	-866
$C_3F_5^+$ (3)	Ne + C_2F_3	-733
$C_4F_4^+$ (2)	Ne + CF_4	-958
$C_3F_4^+$ (12)	Ne + C_2F_4	-788
$C_2F_4^+$ (2)	Ne + C_3F_4	-863
$C_3F_3^+$ (43)	CF_4 + CF_3 + Ne	-1984 - $\Delta_f H°_{298}[C_3F_3^+]$
CF_3^+ (7)	$2C_2F_4$ + F + Ne	-1417

a The majority of the enthalpies of formation at 298 K for ion and neutral species are taken from standard sources.[30,31] Exceptions are the SF_n and SF_n^+ (n =1-5) series,[42] $C_4F_x^+$ (x = 4-5),[33] and $C_3F_5^+$.[43]

b Recombination energy (RE) of reactant ion. For molecular ions, the RE is given for v=0.

c No reaction means the rate coefficient is less than *ca.* 10^{-13} cm^3 $molecule^{-1}$ s^{-1}.

d O^+ was produced *via* CID from N_2O^+, the signal was too small to allow measurement of branching ratios.

e In all reactions forming $C_4F_6^+$, it is assumed to have the linear, rather than the cylic form.

f No $\Delta_f H°_{298}$ value is available for *linear*-$C_4F_5^+$ therefore the value for *c*-$C_4F_5^+$ of –617 kJ mol^{-1} has been used.[33]

Figure Captions

Figure 1 He (I) (University of Southampton) and threshold photoelectron (Daresbury Laboratory) spectra of *c*-C_5F_8. The constant resolutions of the two spectra are 0.05 eV and 0.2 nm, respectively. Note the flat baseline in the threshold spectum for $E <$ *ca.* 12.2 eV, whereas the He (I) spectrum has Franck-Condon intensity over the range 11.2–12.2 eV. (The HTML version of this figure has been enhanced with colour.)

Figure 2 Threshold photoelectron spectrum from the TPEPICO experiment and from a penetrating-field analyzer spectrometer (King *et al*).[37] The resolution of the former spectrum is 0.2 nm, that of the latter 0.005 nm. The spectra are scaled to have the same relative intensity at *ca.* 13 eV. (The HTML version of this figure has been enhanced with colour.)

Figure 3 TPEPICO data for *c*-C_5F_8 over the range 12–22 eV. (a) Threshold photoelectron spectrum recorded on beamline 3.2 of the SRS at a resolution of 0.2 nm and calculated OVGF ionisation energies, (b) ion yield curves recorded on beamline 3.1 at a resolution of 0.3 nm, (c) comparison of SIFT and TPEPICO breakdown diagrams. (The HTML version of this figure has been enhanced with colour.)

Figure 4 Total relative photoion yield for *c*-C_5F_8 from 12.2–22.0 eV recorded on beamline 3.2 with a resolution of 0.2 nm. The insert from 15.5–17.0 eV shows the features due to autoionisation of Rydberg states.

Figure 1

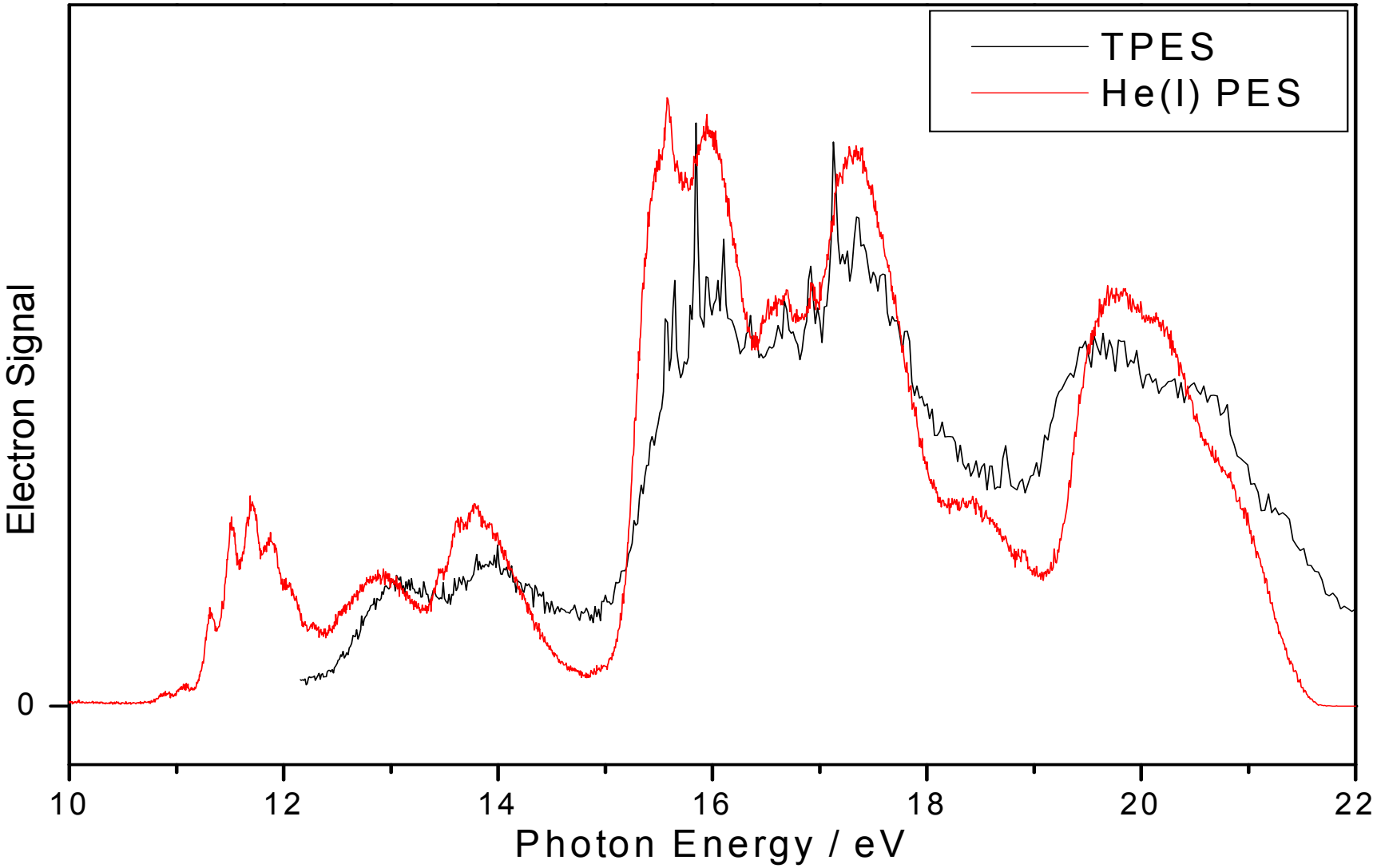
TPES
He(I) PES
Electron Signal
0
10
12
14
16
18
20
22
Photon Energy / eV

Figure 2

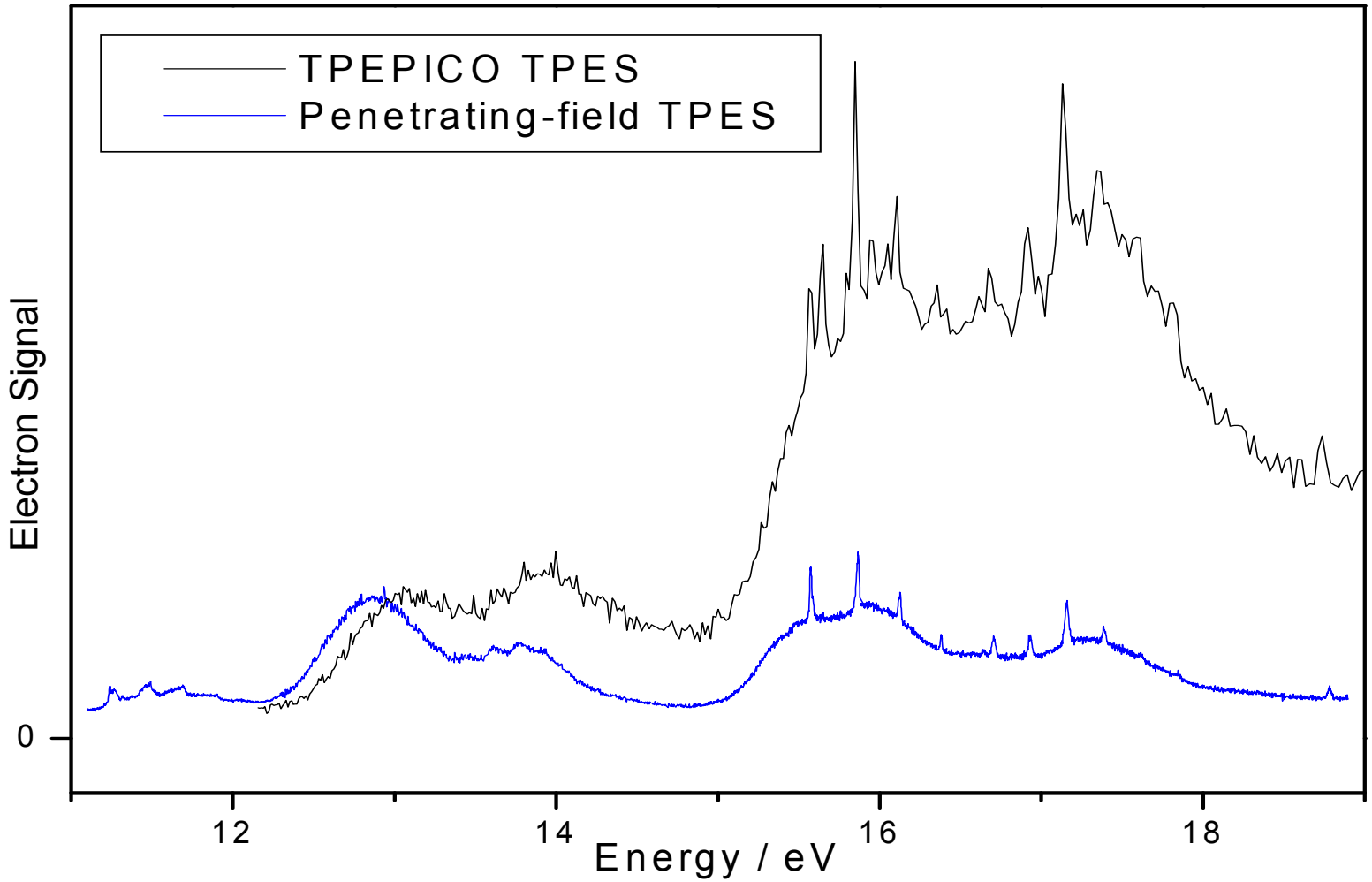
TPEPICO TPES
Penetrating-field TPES
Electron Signal
0
12
14
16
18
Energy / eV

Figure 3

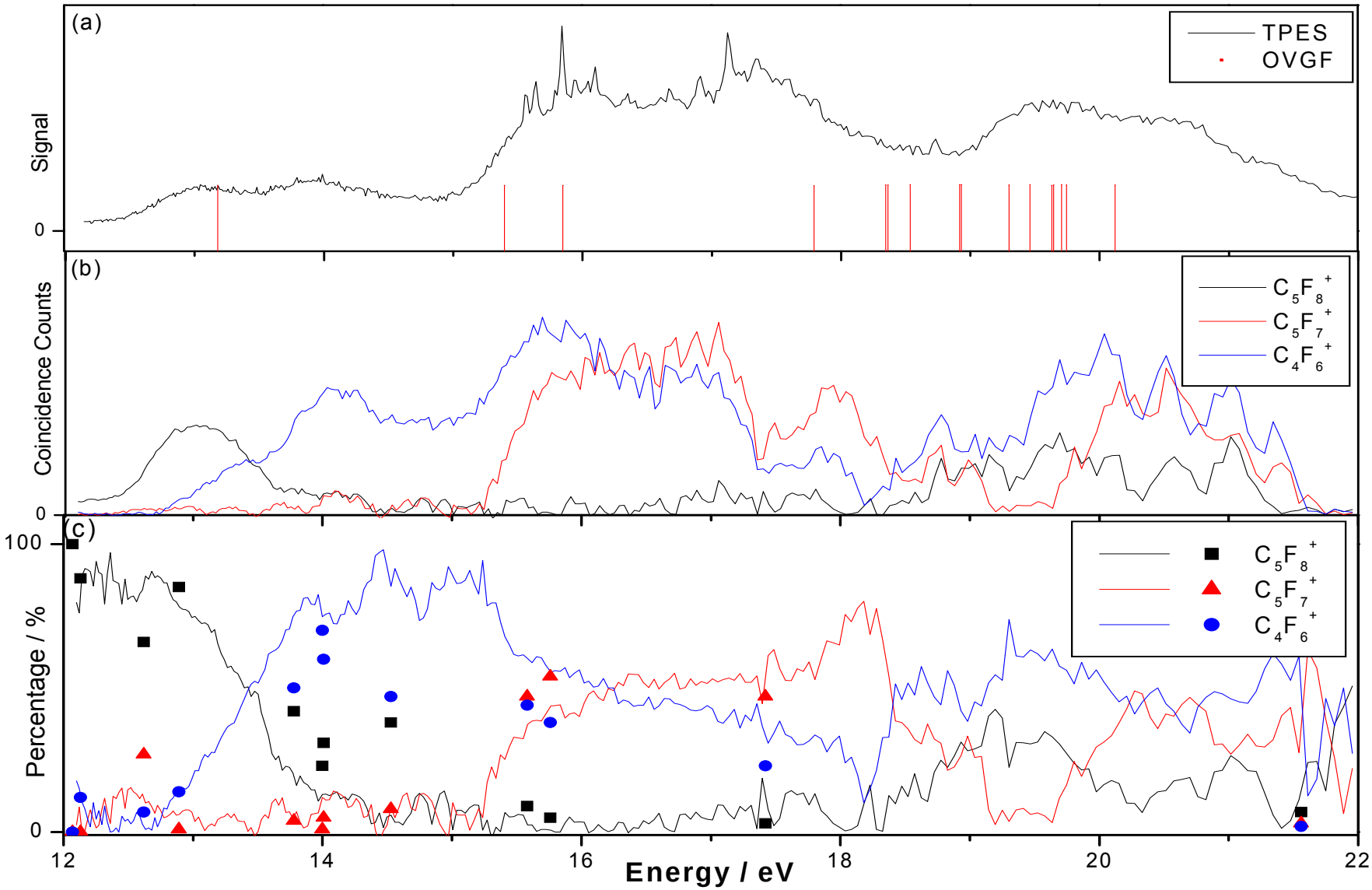
(a)
TPES
OVGF
Signal
0
(b)
Coincidence Counts
$C_5F_8^+$
$C_5F_7^+$
$C_4F_6^+$
0
(c)
100
Percentage / %
0
12
14
16
18
20
22
Energy / eV

Figure 4

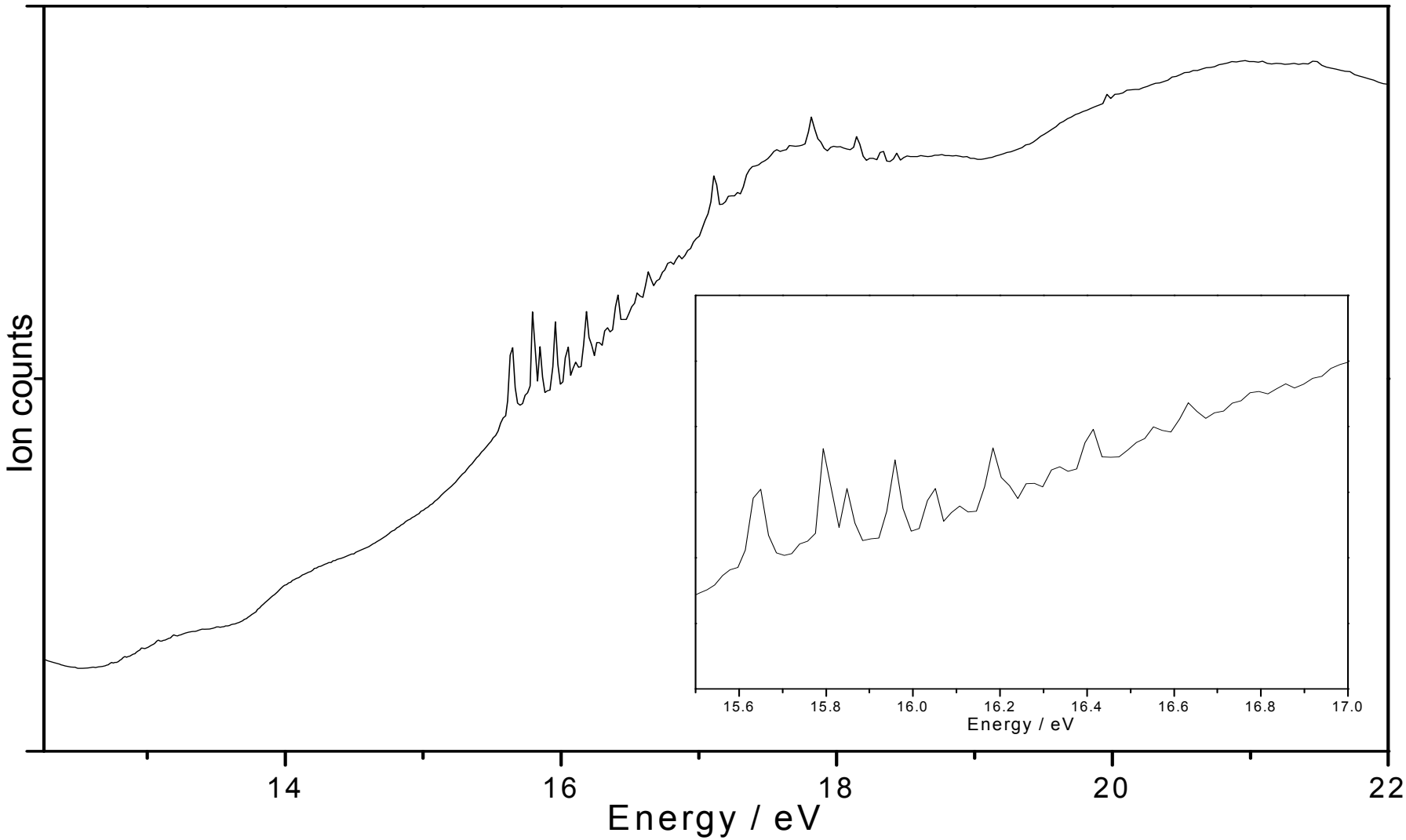
Ion counts
14
16
18
20
22
Energy / eV
15.6
15.8
16.0
16.2
16.4
16.6
16.8
17.0
Energy / eV